

RESEARCH

Open Access



CA916798 predicts poor prognosis and promotes Gefitinib resistance for lung adenocarcinoma

Jian He^{1†}, Xi Lan^{1†}, Xiayan Liu^{1†}, Caixia Deng¹, Hu Luo¹, Yan Wang², Ping Kang³, Zhijian Sun³, Lintao Zhao^{1*} and Xiangdong Zhou^{1*}

Abstract

Background Our previous studies have identified CA916798 as a chemotherapy resistance-associated gene in lung cancer. However, the histopathological relevance and biological function of CA916798 in lung adenocarcinoma (LUAD) remains to be delineated. In this study, we further investigated and explored the clinical and biological significance of CA916798 in LUAD.

Methods The relationship between CA916798 and clinical features of LUAD was analyzed by tissue array and online database. CCK8 and flow cytometry were used to measure cell proliferation and cell cycle of LUAD after knockdown of CA916798 gene. qRT-PCR and western blotting were used to detect the changes of cell cycle-related genes after knockdown or overexpression of CA916798. The tumorigenesis of LUAD cells was evaluated with or without engineering manipulation of CA916798 gene expression. Response to Gefitinib was evaluated using LUAD cells with forced expression or knockdown of CA916798.

Results The analysis on LUAD samples showed that high expression of CA916798 was tightly correlated with pathological progression and poor prognosis of LUAD patients. A critical methylation site in promoter region of CA916798 gene was identified to be related with CA916798 gene expression. Forced expression of CA916798 relieved the inhibitory effects of WEE1 on CDK1 and facilitated cell cycle progression from G2 phase to M phase. However, knockdown of CA916798 enhanced WEE1 function and resulted in G2/M phase arrest. Consistently, chemical suppression of CDK1 dramatically inhibited G2/M phase transition in LUAD cells with high expression of CA916798. Finally, we found that CA916798 was highly expressed in Gefitinib-resistant LUAD cells. Exogenous expression of CA916798 was sufficient to endow Gefitinib resistance with tumor cells, but interference of CA916798 expression largely rescued response of tumor cells to Gefitinib.

[†]Jian He, Xi Lan and Xiayan Liu contributed equally to this work.

*Correspondence:

Lintao Zhao
zhaolintao72@163.com
Xiangdong Zhou
xiangdongzhou2022@163.com

Full list of author information is available at the end of the article



© The Author(s) 2023. **Open Access** This article is licensed under a Creative Commons Attribution 4.0 International License, which permits use, sharing, adaptation, distribution and reproduction in any medium or format, as long as you give appropriate credit to the original author(s) and the source, provide a link to the Creative Commons licence, and indicate if changes were made. The images or other third party material in this article are included in the article's Creative Commons licence, unless indicated otherwise in a credit line to the material. If material is not included in the article's Creative Commons licence and your intended use is not permitted by statutory regulation or exceeds the permitted use, you will need to obtain permission directly from the copyright holder. To view a copy of this licence, visit <http://creativecommons.org/licenses/by/4.0/>. The Creative Commons Public Domain Dedication waiver (<http://creativecommons.org/publicdomain/zero/1.0/>) applies to the data made available in this article, unless otherwise stated in a credit line to the data.

Conclusions CA916798 played oncogenic roles and was correlated with the development of Gefitinib resistance in LUAD cells. Therefore, CA916798 could be considered as a promising prognostic marker and a therapeutic target for LUAD.

Keywords Lung adenocarcinoma, CA916798, CCNB1, G2/M phase, Gefitinib resistance

Background

Lung cancer is the most common malignant tumor and the leading cause of cancer-associated deaths worldwide [1, 2]. Small cell lung cancer and non-small cell lung cancer (NSCLC) are two histopathological types of lung cancer seen in patients clinically. NSCLC accounts for approximately 85% of lung cancer and can be further classified into lung adenocarcinoma (LUAD, 40–50%), lung squamous cell carcinoma (about 30%), and large-cell carcinoma according to histopathological features [3–5]. As the major histological subtypes of NSCLC, LUAD generally evolves from mucosal glands and related with chronic inflammation in lungs [6, 7]. LUAD is one of the most aggressive and rapidly fatal types of cancer with overall survival of less than 5 years for LUAD patients [8, 9]. Despite the progression of chemo-radio therapy, targeted therapy and immunotherapy, the prognosis of LUAD is still poor with 5-year survival less than 15% [10, 11]. The low survival rate is mainly attributed to the primary or acquired resistance to treatments, resulting in progression, metastasis, and recurrence of LUAD [12, 13].

CA916798 gene is firstly identified by our group in a cisplatin-resistant LUAD cell line through suppression cut hybridization technology [14]. CA916798 is expressed at higher levels in the 12-week fetal lung, the 12-week fetal liver and embryonic skin tissues than in normal adult lung tissues in our previous experiments. These results indicate that the CA916798 may be related to embryonic development, which is a characteristic of most tumor-related genes. Indeed, the gene was expressed in a variety of tumor tissues and tumor cells, including lung cancer cells [15–18], prostate cancer cells [19, 20], renal cell carcinoma [21], and breast cancer [22]. Multiple roles of this gene have been reported. For example, our previous work indicated that high CA916798 gene expression was related to cisplatin resistance in LUAD and small cell carcinoma [15, 23, 24]. Accumulating evidence suggests that CA916798 has oncogenic roles. CA916798 is found to be regulated by PI3K/AKT and SHP2 pathways [17, 25, 26], which intensively promote proliferation and inhibit

apoptosis in cancers. CA916798 promotes growth and metastasis of androgen-dependent prostate cancer cells [19]. In addition, C19orf48 encodes a minor histocompatibility antigen in renal cell carcinoma cells [21]. However, the clinical significance and biological function of CA916798 in LUAD remains unclear.

EGFR strongly stimulates cell proliferation, invasion, and metastasis via AKT/MTOR and MAPK/ERK signaling axes [27]. Constitutive activation mutations of EGFR have been frequently detected in LUAD patients, especially in east Asian countries, and these patients are shown to benefit from the first-generation tyrosine kinase inhibitors (TKIs), such as gefitinib and erlotinib [28]. Gefitinib is the most efficient treatment for blocking EGFR activation in clinical cases [29]. However, gefitinib resistance is inevitably developed in most patients [30, 31]. Although different mechanisms of acquired EGFR-TKIs resistance have been reported [32, 33], it remains poorly understood.

In this study, we further explored the functions of CA916798 in LUAD, which demonstrated critical involvements of CA916798 in poor prognosis of LUAD and revealed CA916798 as a promising target for in Gefitinib-resistant LUAD.

Methods

Cell lines and reagents

A549, PC9 and HCC827 human LUAD cell lines (Shanghai Institute of Biochemistry and Cell Biology, Shanghai, China) were cultured in DMEM containing 10% fetal bovine serum (FBS) (16,140,071, ThermoFisher Scientific, Shanghai, China) at 37 °C and 5% CO₂. Ro-33,066, Gefitinib, and sodium carboxymethyl cellulose (CMC-Na) was purchased from Selleck (Houston, TX, USA).

Lentivirus, infection, and stable cell lines

Three short hairpin RNAs (shRNAs) targeting CA916798 and mock shRNA were inserted into lentivirus by GenePharma (Shanghai, China). The shRNA target sequences are listed in Table 1. Lentivirus containing human full-length CA916798 or empty vector as control were constructed by GenePharma (Shanghai, China). Lentivirus was used to infect cells following standard protocols and cells were selected using 5 µg/mL puromycin (Sigma, USA).

Table 1 Sequences of CA916798 shRNA control shRNA.

Plasmid	Sequence
LV3-Ctrl	TTCTCCGAACGTGTCACGT
LV3-CA916798-Homo-1	TGGAGGCCGCTTGGAGAT
LV3-CA916798-Homo-2	GACCCAACCCAGTGCAAGG
LV3-CA916798-Homo-3	TCCATACGCCACCGTGAGA

Immunohistochemistry (IHC)

LUAD tissue microarray (HLugA180Su06) was purchased from Shanghai Outdo Biotech CO., LTD. (<http://www.superchip.com.cn/index.html>). IHC of tissue array and tumor xenografts was performed using the streptavidin-biotin peroxidase complex method and a rabbit polyclonal antibody against CA916798 (1:100, Invitrogen, USA). Photographs were obtained using an Olympus BX51 microscope and expression was scored in five random fields using the Image-Pro Plus 5.0 software. The area sum and integrated optical density (IOD) sum of the positive-stained sites (brown staining) were measured in pixels. CA916798 expression intensity was determined as the mean value of IOD sum/area sum in five images per slide. The same parameter settings were maintained for all images. Combined with the clinical prognosis of patients, the cut-off value for expression was 0.027609, as analyzed with SPSS 22.0. Expression > 0.027609 was defined as CA916798 high expression.

RNA extraction and quantitative real-time RT-PCR

Total RNA was extracted using the RNAfast200 Kit (Feijie, Shanghai, China) and the PrimeScript RT Master Mix (Takara, Japan) was used for reverse transcription according to the manufacturers' instructions. qRT-PCR reactions were conducted with the SYBR Premix Ex Taq II (Takara) on the Bio-Rad CFX96 Real-Time PCR Detection System (Bio-Rad, USA) in accordance with the manufacturers' instructions. qRT-PCR was performed in triplicate. β -actin mRNA expression was used for normalization. The qRT-PCR primers are listed in Table 2.

Western blot analysis

Cells were lysed in RIPA buffer (Thermo, USA) containing 1% protease and phosphatase inhibitors following the manufacturer's protocol. Lysates were incubated with SDS-PAGE Sample Loading Buffer (Bio-Rad, USA) for 10 min at 95 °C. Proteins were separated by 10% SDS-PAGE and transferred to a PVDF membrane (Bio-Rad, USA). After blocking in 5% non-fat milk for 2 h, the membrane was incubated at 4 °C overnight with the following primary antibodies: CA916798 (1:100, Invitrogen, USA), β -actin (1:5000, CST, USA), WEE1 (1:500, CST, USA), CDK1 (1:1000, CST, USA), p-CDK1Y15 (1:500, CST, USA), and CCNB1 (1:500, CST, USA).

Cell invasion and migration assays

Transwell inserts (8.0 μ m pore; Millipore, USA) were precoated with Matrigel (for invasion assays) or left untreated (for migration assays) and placed into 24-well plates. Cells were seeded into the upper chambers (5×10^4 /well) with 200 μ L serum-free medium and 600 μ L DMEM medium containing 10% FBS was added to the lower chambers. Cells were incubated for 36 h and 24 h for invasion and migration assays, respectively. Cells were then fixed in 4% paraformaldehyde and dyed with crystal violet. Five random fields were examined for each chamber, and the invaded or migrated cells were counted. Images were obtained using a light microscope at 100-fold magnification.

Colony formation assay

Cells were seeded into 6-well plates at a density of 200 cells per well. Plates were then incubated at 37 °C with 5% CO₂ for 10–14 days until colonies were visible. Plates were washed with phosphate buffer saline (PBS) and 4% paraformaldehyde was used to fix cells for 15 min. Colonies were stained with crystal violet solution for 15 min, followed by a wash in PBS and air-drying, five random fields were selected for each well and colonies were counted. Images were obtained using a light microscope at 100-fold magnification.

Cell viability and flow cytometric analysis

Cells were seeded in a 96-well plate (1000 cells per well). Cell viability was measured over 7 days using the CCK8 Kit (Beyotime, Shanghai, China), according to the manufacturer's instruction. The Cell Cycle and Apoptosis Analysis Kit (Beyotime, Shanghai, China) was used to determine cell cycle distribution following the manufacturer's instructions.

Animal experiments

Six-week-old female NOD/SCID mice were obtained from Charles River Labs (Beijing, China) and kept in specific pathogen-free conditions with light/dark cycles of 12 h, 60% humidity, 23 ± 3 °C, and free access to water. The mice were randomly divided into two groups: shRNA-CA916798, shRNA-control (n = 5 per group). The mice were anesthetized with an intraperitoneal injection of pentobarbital (50 mg/kg). No signs of peritonitis, pain, or discomfort were observed after anesthesia. The indicated cells were subcutaneously injected into mice (1×10^6 cells per mouse). Tumor size was measured at days 15, 20, 24 and 28. For treatment, the Gefitinib and vehicle was given through gavage administration Qod for total 14 days. The mice were euthanized by cervical dislocation at 28 days after implantation. Tumors were fixed in formaldehyde and subjected to paraffin embedding for hematoxylin and eosin and IHC staining. The animal

Table 2 Primer sequences used in the experiments

Gene symbol	Primer sequence
CA916798	Forward: 5'-TTCTCCGAACGTGTACACGT-3'
CA916798	Reverse: 5'-TGGAGGCCGTCTTGGAGAT-3'
ACTB	Forward: 5'-CATGTACGTTGCTATCCAGGC-3'
ACTB	Reverse: 5'-CTCCTTAATGTCACGCACGAT-3'

experiments were approved by the Laboratory Animal Welfare and Ethics Committee of Army Medical University (AMUWEC20182181).

Statistical analysis

All experiments were repeated at least three times and each treatment was set up in triplicate, unless specially indicated otherwise. Data are presented as mean \pm SD. Statistical analyses were performed using SPSS version 24.0 and GraphPad Prism 5, String Version 11.0 by a two-tailed Student's t-test. The cut-off value of CA916798 IHC staining scores was analyzed with SPSS. Chi-square analysis was used to evaluate the relationship between CA916798 high rate and LUAD clinicopathological features. $P < 0.05$ indicated statistical significance. High and low expression of genes were defined using median value. TCGA_LUAD mRNA expression and methylation450K datasets were downloaded from <https://xenabrowser.net>. Gene Set Enrichment Assay (GSEA) ($P < 0.05$, FDR < 0.25) [34] were used to analyze data. The statistical significance was determined by Student's t test and $P < 0.05$ was considered statistically significant. Kaplan-Meier survival plot and log-rank statistics were used to evaluate the survival of patients. Pearson rank correlation was used to analyze the relationship between different genes or proteins.

Results

CA916798 overexpression predicted poor prognosis for LUAD patients.

We first examined protein expression of CA916798 in 94 LUAD tumors and 86 matched non-tumor tissues by IHC. The result indicated that CA916798 was barely detected in non-tumor lung tissues (Fig. 1A) but strongly expressed in tumor cells of LUAD (Fig. 1B). Statistic data suggested that CA916798 expression was significantly higher in tumor tissues than in adjacent non-tumor tissues (Fig. 1C). The expression of CA916798 was correlated with tumor T-stage (Fig. 1D), but not with sex, age, N-stage, M-stage, and pathological grade (**data not shown**). Moreover, patients with high CA916798 expression showed significantly shorter overall survival time than those with low CA916798 expression (Fig. 1E). To examine the results afore mentioned, we analyzed TCGA_LUAD dataset (gene expression RNAseq) and consistently observed the upregulation of CA916798 in tumor tissues compared with non-tumor lung tissues (Fig. 1F) and worse prognosis of patients with high CA916798 than those with low CA916798 (Fig. 1G). Analysis on Lung Cancer database from Kaplan-Meier plotter (<https://kmpplot.com>) also proved that high expression of CA916798 was associated with shortened overall survival time of LUAD patients (Fig. 1H). Since CpG island methylation in gene promoter region has

been known to be critically regulate gene expression, we analyzed the TCGA_LUAD methylation 450 K dataset. The result showed that several methylation probes were localized in the promoter of CA916798 gene and the one closely next to transcription start site (probe cg22306691) had significantly negative correlation with mRNA level of CA916798 (Fig. 1I). In addition, the methylation level of cg22306691 was also dramatically downregulated in LUAD tissues compared to adjacent non-tumor tissues (Table 3). Moreover, low methylation level of probe cg22306691 predicted poor prognosis (Fig. 1K). Therefore, the expression of CA916798, partially regulated by promoter methylation, was correlated with tumor progression and predicted poor prognosis of LUAD.

CA916798 promoted growth of LUAD cells *in vitro* and *in vivo*.

We then explored the biological function of CA916798 in LUAD cells. For this purpose, CA916798 was stably knocked down in A549 and PC9 cell lines using shRNA targeting CA916798 (A549-shCA916798 and PC9-shCA916798) with scramble shRNA as control (A549-shCtrl and PC9-shCtrl) (Fig. 2A). CCK8 assay and colony formation assay indicated that CA916798 knockdown significantly impaired cell viability and growth (Fig. 2B C). However, transwell assay suggested that CA916798 knockdown did not affect cell migration (seeding cells without Matrigel) and invasion (seeding cells with Matrigel) of A549 and PC9 cells (Fig. 2D and E). To further examine the effects of CA916798 on cell growth of LUAD *in vivo*, we generated a subcutaneous xenograft model using A549-shCA916798 cells and A549-shCtrl cells. The result suggested that CA916798 knockdown suppressed tumorigenicity of A549 cells in nude mice (Fig. 2F H). Hematoxylin-eosin (HE) staining and Ki67 staining confirmed that CA916798 deficiency markedly reduced growth of A549 cells *in vivo* (Fig. 2I). Together, these results suggested that interference of CA916798 expression impaired cell growth of LUAD *in vitro* and *in vivo*.

CA916798 was involved in regulation on G2/M phase transition in LUAD cells.

To further pursue the mechanism on the regulation of LUAD cell growth by CA916798, we examined the effect of CA916798 on cell cycle of LUAD cells through flow cytometric analysis. The result showed that CA916798 knockdown in two LUAD cell lines consistently induced G2/M phase arrest (Fig. 3A and B). GSEA [34, 35] on TCGA_LUAD dataset suggested that high expression of CA916798 significantly enriched HALLMARK_G2M_CHECKPOINT geneset (Fig. 3C). It is known that CCNB1 is the critical checkpoint for G2/M phase [36], and analysis on TCGA_LUAD dataset revealed that CCNB1 was the most correlated gene with CA916798 among all cyclin genes (Fig. 3D and Table 4).

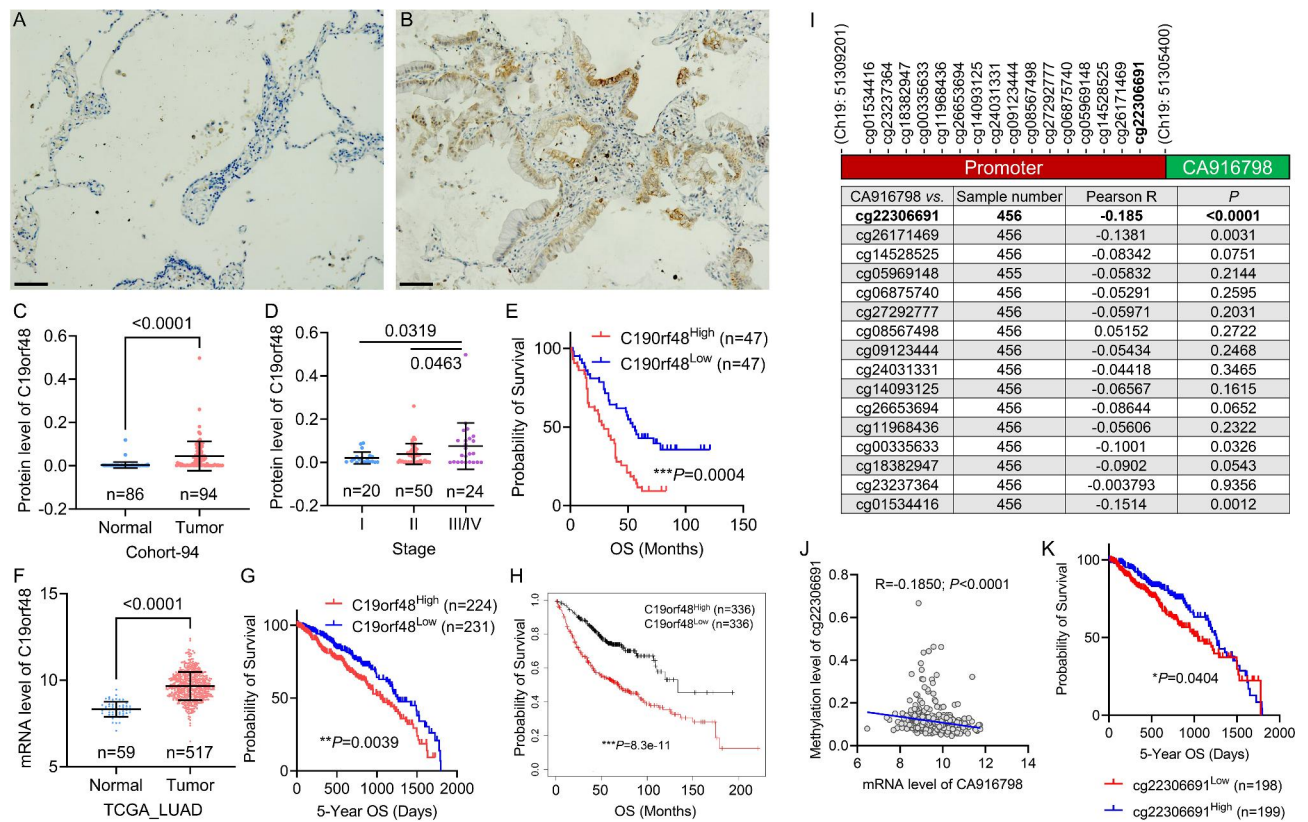


Fig. 1 CA916798 is upregulated in LUAD and predicts poor survival of patients

A and B) Representative IHC images of CA916798 in matched non-tumor tissue (A) and LUAD tissue (B). Scale bar = 100 μm. Brown color represents CA916798 protein; blue color represents nuclei

C) IHC score of CA916798 expression in matched non-tumor tissue (Normal) and LUAD tissue (Tumor) from Cohort-94. Data are shown as mean ± SD.

D) IHC score of CA916798 expression in different stages of LUAD from Cohort-94. Data are shown as mean ± SD.

E) Kaplan-Meier analysis on overall survival (OS) in LUAD patients with CA916798^{high} vs. CA916798^{low} from Cohort-94

F) mRNA level of CA916798 in matched non-tumor tissue (Normal) and LUAD tissue (Tumor) from TCGA_LUAD dataset. Data are shown as mean ± SD.

G) Kaplan-Meier analysis on 5-year overall survival (OS) in LUAD patients with CA916798^{high} vs. CA916798^{low} from TCGA_LUAD dataset

H) Kaplan-Meier analysis on overall survival (OS) in LUAD patients with CA916798^{high} vs. CA916798^{low} from KM-PLOT-LUAD database

I) Pearson correlation list of methylation levels with CA916798 mRNA expression in TCGA_LUAD mRNA and methylation450K datasets

J) Pearson correlation of CA916798 with cg22306691 from TCGA_LUAD mRNA and methylation450K datasets

K) Kaplan-Meier analysis on 5-year overall survival (OS) in LUAD patients with cg22306691^{high} vs. cg22306691^{low} from TCGA_LUAD methylation450K dataset

These findings indicated that CA916798 might regulate the G2/M phase transition in LUAD cells, and silencing CA916798 could suppress tumor growth by inducing G2/M phase arrest.

CA916798 activated the WEE1/CDK1 axis to promote cell cycle progression.

It is well-known that the CDK1/CCNB1 complex promotes cell cycle progression from G2 phase to M phase and results in cell proliferation [37, 38]. WEE1 inactivates the CDK1/CCNB1 complex by phosphorylating CDK1 at Tyr15 amino acid. Conversely, CDC25C activates the CDK1/CCNB1 complex by dephosphorylate CDK1 at the Tyr15 [37, 38]. Pearson correlation on TCGA_LUAD dataset revealed significantly positive correlation of CA916798 and CDK1 (Fig. 4A). Moreover, protein levels of p-CDK1(Tyr15) and WEE1 were upregulated upon

interference of CA916798 in A549 and PC9 cells (Fig. 4B). On the contrary, overexpression of CA916798 reduced protein levels of p-CDK1(Tyr15) and WEE1 (Fig. 4C). These findings suggested that CA916798 might promote proliferation of LUAD cells by inhibiting the expression of WEE1 and the phosphorylation of CDK1(Tyr15). Next, we treated A549 cells with CDK1 inhibitor Ro-33,066 (5 μM for 24 h) and the data indicated that CDK1 inhibitor led to G2/M phase arrest in both A549-Control and A549-CA916798 cells (Fig. 4D). Therefore, CA916798 could promote cell proliferation through regulating WEE1/CDK1 axis.

CA916798 was correlated with Gefitinib sensitivity.

For LUAD, TKI targeting EGFR, such as Gefitinib, promotes G2/M phase arrest to inhibit tumor growth but fails to do so in TKI resistant cells. Thus, we asked

Table 3 Average methylation level of LUAD vs. matched normal tissues in TCGA.

Probe	Average methylation level		LUAD:Normal	P
	Normal (n=32)	LUAD (n=456)		
cg22306691	0.1336	0.1122	0.8400	0.0009
cg26171469	0.1451	0.1425	0.9822	0.5224
cg14528525	0.0331	0.0315	0.9522	0.3985
cg05969148	0.1422	0.1275	0.8964	0.0003
cg06875740	0.1059	0.0898	0.8479	0.1407
cg27292777	0.0211	0.0209	0.9919	0.9088
cg08567498	0.0768	0.0750	0.9758	0.5768
cg09123444	0.0594	0.0568	0.9571	0.3367
cg24031331	0.0765	0.0800	1.0459	0.0915
cg14093125	0.0539	0.0508	0.9413	0.2544
cg26653694	0.0701	0.0666	0.9494	0.3165
cg11968436	0.0615	0.0579	0.9410	0.2271
cg00335633	0.0957	0.0947	0.9899	0.7703
cg18382947	0.1278	0.1253	0.9802	0.5676
cg23237364	0.0306	0.0332	1.0860	0.2523
cg01534416	0.2769	0.2327	0.8404	0.0001

whether CA916798 could facilitate resistance of LUAD cells against Gefitinib. To this aim, we developed Gefitinib-resistant PC9 (PC9/R) and HCC827 (HCC/R) cells through culturing the cells in the presence of Gefitinib with gradually increased concentrations. CCK8 assay showed that IC₅₀ of parental PC9 and PC9/R cells for Gefitinib were 0.028 μM and 8 μM, respectively, and IC₅₀ of parental HCC827 and HCC/R cells for Gefitinib were 0.141 μM and 18.27 μM, respectively (Fig. 5A), confirming successful establishment of Gefitinib-resistant cells. Through qRT-PCR, we found that the mRNA level of CA916798 was significantly upregulated in Gefitinib-resistant cells compared with parental cells (Fig. 5B), implying potential implication of CA916798 in acquired Gefitinib resistance. Consistent with our result, analysis on data from GEO dataset GSE34228 also showed that CA916798 expression was increased in PC9/R cells compared with PC9 parental cells (Fig. 5C). In GSE172002, the expression of CA916798 in HCC827/R cells was also higher than that in HCC827 parental cells (FPKM value 56.89 vs. 35.63). However, the analysis on GSE200894 indicated that the sensitivity of PC9 cells to the third-generation TKI, osimertinib, was not associated with CA916798 expression (Fig. 5D). To verify whether CA916798 participated in the regulation of LUAD response to Gefitinib, PC9/R and HCC/R cells were stably infected by lentivirus including shRNA targeting CA916798 (PC9/R-siCA and HCC/R-siCA) or control shRNA (PC9/R-siCtrl and HCC/R-siCtrl) (Fig. 5E F). Notably, knockdown of CA916798 in Gefitinib-resistant cells significantly decreased IC₅₀ against Gefitinib from 10.34 μM to 3.92 μM ($P < 0.01$) in PC9/R cells and from 14.1 μM to 8.07 μM ($P < 0.05$) in HCC/R cells, respectively

(Fig. 5E F). Furthermore, forced expression of CA916798 in parental PC9 and HCC827 cells increased IC₅₀ of the cells against Gefitinib from 0.48 μM to 2.60 μM ($P < 0.01$) in PC9 cells and from 0.06 μM to 1.42 μM ($P < 0.001$) in HCC cells, respectively (Fig. 5G H). Therefore, CA916798 was tightly associated with development of Gefitinib resistance in LUAD cells.

CA916798 knockdown promoted inhibitory effects of Gefitinib *in vivo*.

Since overexpression of CA916798 dampened effects of Gefitinib on LUAD cells, we then examined whether interference of CA916798 expression would enhance Gefitinib inhibitory effects. For this purpose, we established a xenograft model through subcutaneously inoculated PC9/R-shCA916798 or PC9/R-shCtrl cells into NOD/SCID mice followed by treatment of Gefitinib or placebo (Fig. 6A). Consistent with *in vitro* results, CA916798 knockdown significantly inhibited the growth of xenograft (Fig. 6B). Both tumor volume and tumor weight were decreased with knockdown of CA916798 (Fig. 6C and D). Moreover, Gefitinib showed stronger inhibitory effects on PC9/shCA916798 cells than PC9/shCtrl cells (Fig. 6B and D). HE staining indicated that in Gefitinib treatment did not obviously change pathological features of PC9/shCtrl cells and only slightly decreased density tumor cells (Fig. 6E). However, Gefitinib treatment induced significant death of tumor cells and collapse of nuclei (Fig. 6E), confirmed the inhibitory effects of Gefitinib on LUAD cells with knock down of CA916798. Therefore, diminishing CA916798 might augment inhibitory effects of Gefitinib on LUAD cells.

Discussion

In this study, we explored the clinicopathological significance of CA916798 in LUAD and found that CA916798 expression was significantly correlated with poor prognosis of LUAD patients. Surprisingly, our study also identified a key methylation site in promote region of CA916798 gene as a mechanic regulator for CA916798 gene expression and clinical predictor for patient prognosis of LUAD. Through cell and animal experiments, we further delineated that CA916798 promoted proliferation and tumorigenesis of A549 cells. In addition, CA916798 was upregulated in Gefitinib-resistant LUAD cells and elimination of CA916798 facilitated Gefitinib effects on LUAD cells (Fig. 7).

The occurrence and development of NSCLC is a complex process involving multiple abnormal gene expression and mutation. EGFR-tyrosine kinase inhibitors have opened up a new era of treatment in NSCLC [39, 40]. Subsequent drugs targeting ALK, ROS1, KRAS, BRAF, MET, RET, NTRK, and other genes have also been explored [41]. As more genes related to lung cancer are discovered, more targeted drugs will enter clinical

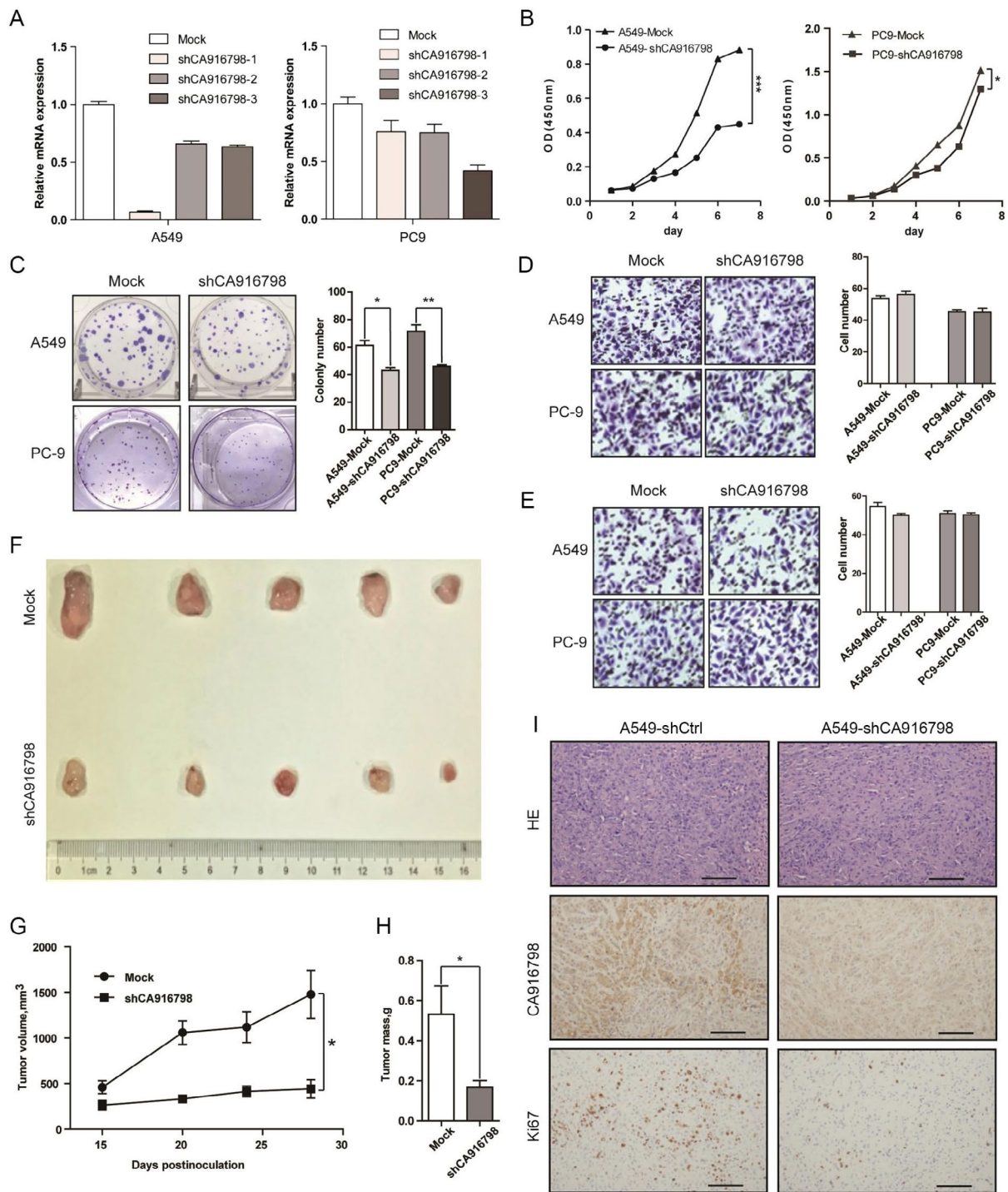


Fig. 2 CA916798 promotes growth of LUAD cells *in vitro* and *in vivo*

A) The efficiency of CA916798 knockdown in A549 and PC9 cells with three individual shRNA sequence targeting CA916798. shCA916798-1 and –3 are used in A549 and PC9, respectively, for the following experiments

B) Growth curve of CA916798-knockdown LUAD cells and mock cells as measured by CCK8 assay. Data are shown as mean ± SD (n=3; *P<0.05, ***P<0.001)

C) Colony formation of CA916798-knockdown LUAD cells and mock cells. Data are shown as mean ± SD (n=3; *P<0.05, ** P<0.01)

D and E) Measurement on migration (D) and invasion (E) in CA916798-knockdown cells and mock cells. Data are shown as mean ± SD (n=3)

F-H) Tumor image (F), tumor volume (G), and tumor weight (H) of xenograft models generated using A549-shCA916798 and mock cells. Data are shown as mean ± SD (n=5; *P<0.05)

I) HE and IHC staining of tumor tissues from experimental mice obtained 28 days after implantation

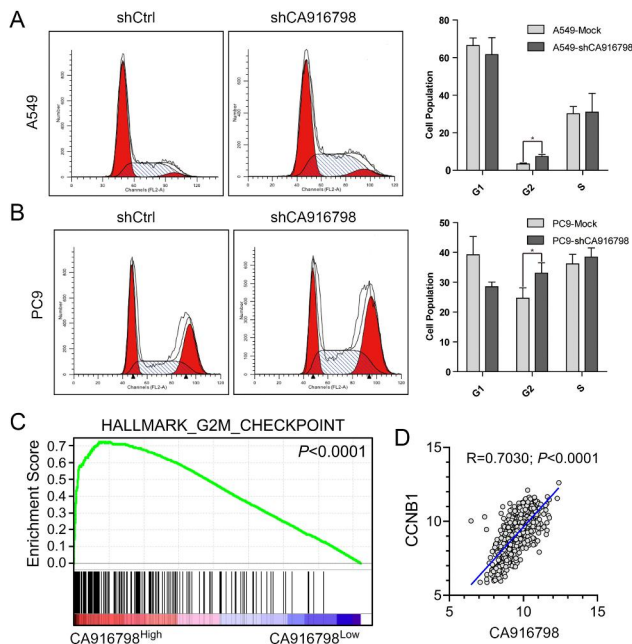


Fig. 3 CA916798 regulates G2/M-phase transition in LUAD cells

- A)** Cell cycle analysis in CA916798-knockdown LUAD cells and mock cells (**P* < 0.05)
- B)** Cell cycle analysis in CA916798-overexpressing LUAD cells and mock cells (**P* < 0.05)
- C)** Geneset enrichment assay on TCGA_LUAD dataset
- D)** Pearson correlation of CA916798 with CCNB1 from TCGA_LUAD dataset

Table 4 Pearson correlation of CA916798 with cyclin genes

Correlation of CA916798	Pearson R	P Value
vs. CCNB1	0.703	<0.0001
vs. CCNB2	0.6812	<0.0001
vs. CCNA2	0.6256	<0.0001
vs. CCNE1	0.5929	<0.0001
vs. CCNE2	0.5215	<0.0001
vs. CCNO	0.286	<0.0001
vs. CCNI2	0.1826	<0.0001
vs. CCNC	0.1711	<0.0001
vs. CCNT2	-0.00597	0.8863
vs. CCNH	-0.01291	0.7572
vs. CCNG2	-0.01784	0.6692
vs. CCNA1	-0.1075	0.0098
vs. CCNT1	-0.1118	0.0072
vs. CCNG1	-0.1145	0.006
vs. CCND1	-0.1427	0.0006
vs. CCNI	-0.1722	<0.0001
vs. CCNB3	-0.1939	<0.0001
vs. CCND3	-0.2588	<0.0001
vs. CCND2	-0.3642	<0.0001

application, expanding the treatment possibilities for lung cancer patients.

The CA916798 gene was identified more than 10 years ago, but the function of its encoded protein is still obscure. It is found that the CA916798 gene encodes a

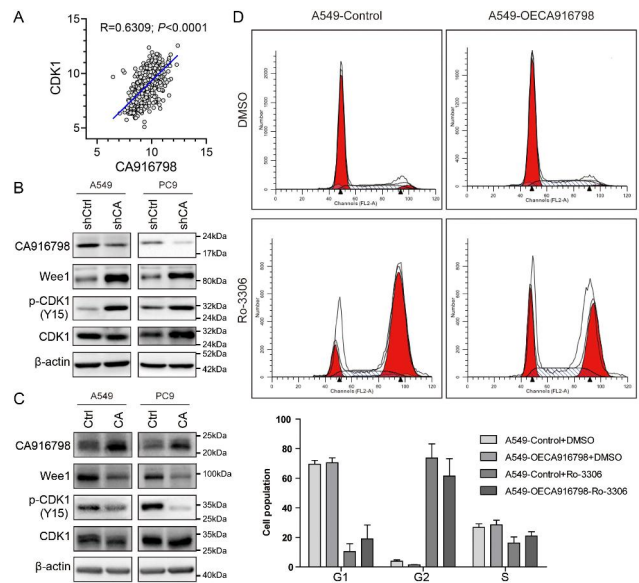


Fig. 4 CA916798 activates WEE1/CDK1 axis to promote cell cycle progression

- A)** Pearson correlation of CA916798 with CDK1 from TCGA_LUAD dataset
- B)** Western blotting of A549 and PC9 cells with CA916798 knockdown (shCA) vs. shControl (shCtrl)
- C)** Western blotting of A549 and PC9 cells with CA916798 overexpression (CA) vs. empty vector (Ctrl)
- D)** Cell cycle distribution measured by flow cytometry in cells treated with 0.1 μM Ro-3306 (CDK1 inhibitor) for 24 h

minor histocompatibility antigen, which is presented to cytotoxic T cells and initiates killing effects on tumor cells in patients with renal cancer [21]. The CA916798-encoded antigen is expressed in a variety of tumor cells, so it may be related to tumor immunity. However, this possibility remains to be investigated. We previously reported that the CA916798 gene is related to chemotherapy resistance in lung cancer; a higher the expression of this gene was associated with a higher chemotherapy resistance. Further studies showed that the gene is regulated by the PI3K/AKT signaling axis, which regulates the proliferation and apoptosis of malignant tumors. Therefore, CA916798 gene might be a lung cancer-related gene and represent a promising therapeutic target for LUAD treatment.

Cell proliferation is tightly regulated by a cell cycle network, including cyclin proteins, cyclin-dependent protein kinases, and cyclin-dependent protein kinase inhibitors. G1/S and G2/M boundaries are the most important checkpoints in cell cycle regulation. Our results showed that CA916798 influenced the expression of WEE1 and CDK1, which are key molecules that regulate the G2/M transition. It is clear that CDK1 binds to CCNB1 as a mitotic promoter that drives G2 to M phase transition. The mitotic promoter complex is inactive due to phosphorylation of Thr14 and Tyr15 of CDK1 by WEE1. We found that CA916798 inhibited the expression of WEE1

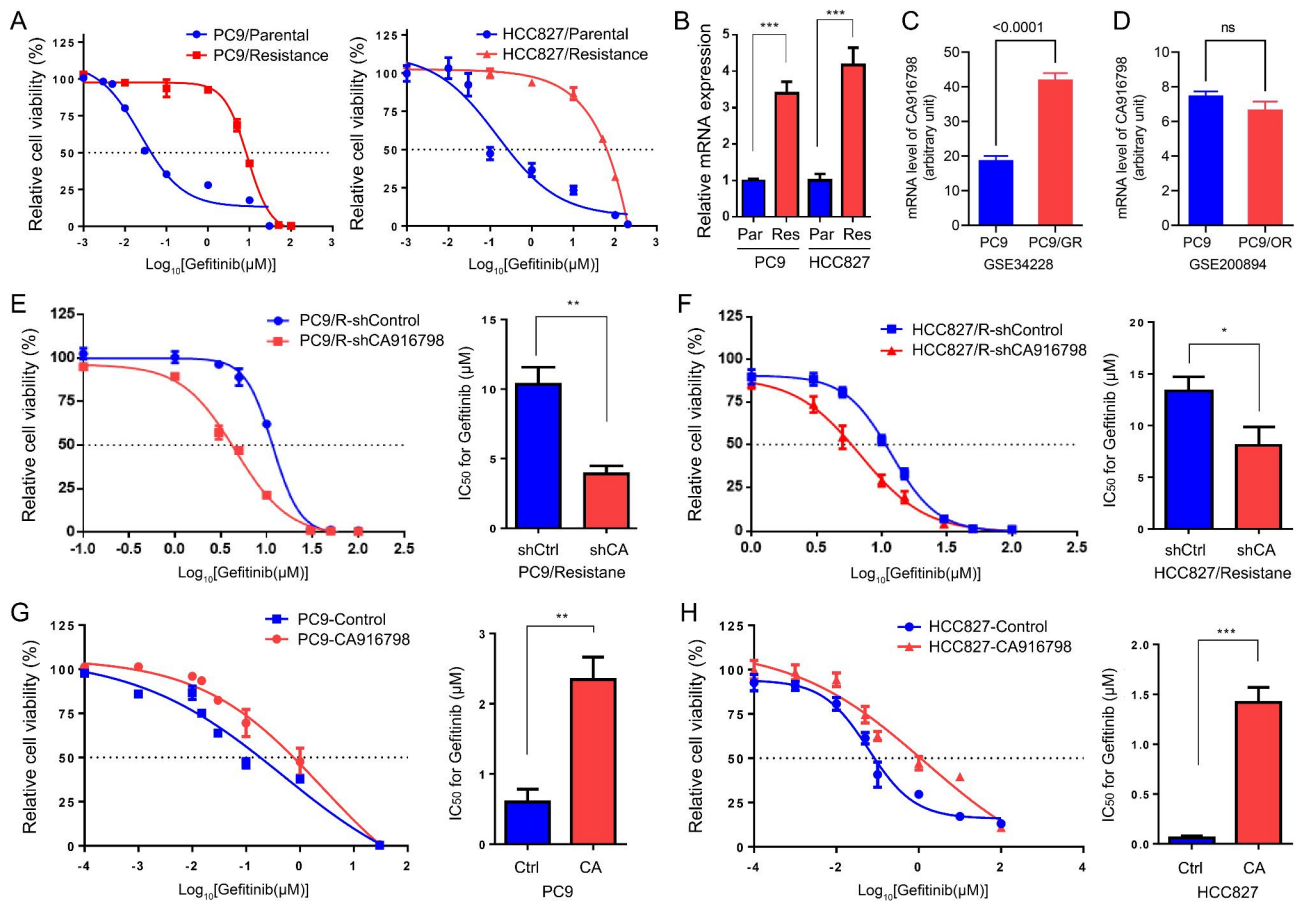


Fig. 5 Correlation of CA916798 with Gefitinib sensitivity in LUAD cells

A) Cell growth curves of parent and Gefitinib-resistant cells from PC9 and HCC827 measured via CCK8.
B) mRNA level of CA916798 in parent and Gefitinib-resistant cells from PC9 and HCC827 measured via qRT-PCR. *** $P < 0.001$
C) mRNA level of CA916798 in PC9 and PC9/GR (Gefitinib resistance) cells
D) mRNA level of CA916798 in PC9 and PC9/OR (Osimertinib resistance) cells
E and F) Cell growth curves with Gefitinib treatment and IC_{50} calculation of Gefitinib for PC9/Resistance (**E**) and HCC827/Resistance (**F**) cells stably transfected with control shRNA (shCtrl) or shRNA targeting CA916798 (shCA). ** $P < 0.01$
G and H) Cell growth curves with Gefitinib treatment and IC_{50} calculation of Gefitinib for PC9 (**G**) and HCC (**H**) cells stably transfected with empty vector (Ctrl) or CA916798 (CA). ** $P < 0.01$, *** $P < 0.001$

in LUAD cells, suggesting that CA916798 might be a transcriptional repressor of WEE1. Reduction of WEE1 promotes dephosphorylation and activation of CDK1 and eventually leads to cell cycle progression. These findings indicated that CA916798 promoted cell proliferation through regulation of WEE1/CDK1.

EGFR-TKI inhibits cell proliferation by competitively binding to ATP binding sites in the catalytic domain of tyrosine kinase, inhibiting its self-phosphorylation and blocking downstream signal transduction. In vivo, Gefitinib and other EGFR-TKI drugs widely inhibit the tumor growth of human tumor cell derived lines xenografted in nude mice, and improve the anti-tumor activity of chemotherapy, radiotherapy and hormone therapy. Our data firstly reported that knockdown of CA916798 improved the sensitivity of drug-resistant cells to EGFR-TKI and enhanced the growth inhibition of EGFR-TKI on NSCLC

cells. LUAD cell derived xenograft in immunodeficient NOD/SCID mice further established that knockdown of CA916798 combined with TKI significantly inhibited tumor growth compared with single drug treatment. These findings suggested that the increased expression of CA916798 significantly promoted the development of EGFR TKIs resistance, so CA916798 might be an important molecule to promote the acquired EGFR TKIs resistance of LUAD cells. However, it should be mentioned that Gefitinib is a first-generation TKI, while Osimertinib is a third-generation TKI. Our current finding, in association with other reports, emphasized that CA916798 is associated with Gefitinib but not Osimertinib resistance. Since first-generation TKIs block EGFR activity through reversible interaction, CA916798 might lead to Gefitinib resistance through interference with the interaction between EGFR and Gefitinib. However, third-generation

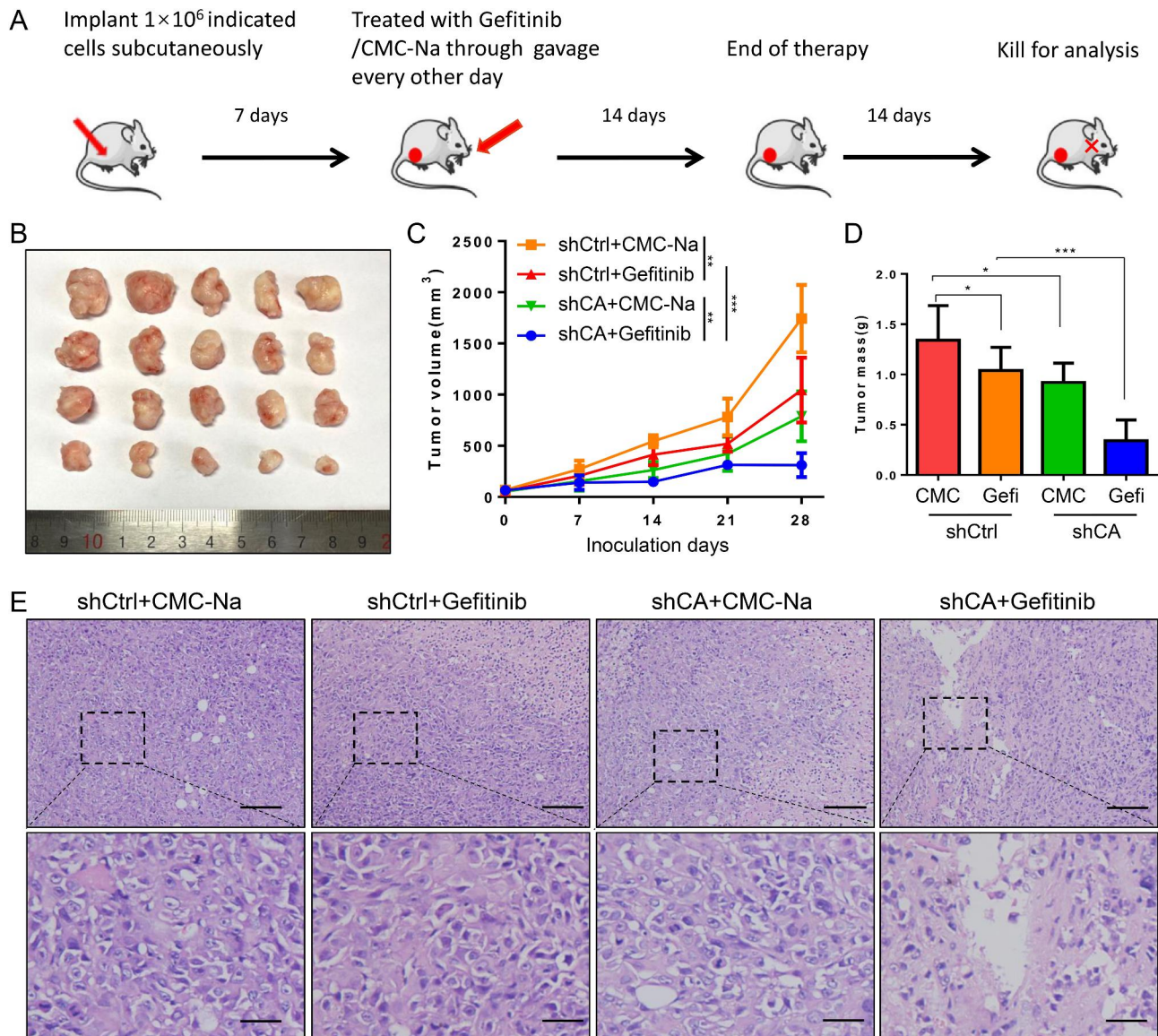


Fig. 6 Targeting CA916798 enhances Gefitinib inhibitory effects on LUAD cells

A) Flow chart of in vivo experiment. CMC-Na is used as control for Gefitinib

B-D) Tumor image (B), tumor volume (C), and tumor weight (D) of xenograft models generated using PC9/GR cells stably transfected with control shRNA (Mock) or shCA916798 treated with CMC-Na or Gefitinib. Data are shown as mean \pm SD (n = 5, * $P < 0.05$, *** $P < 0.001$)

E) Representative HE staining of xenograft tumors. Scale bar = 100 μm (upper panels) or 25 μm (lower panels)

TKIs specifically target mutant EGFR, which could not be affected by CA916798 function. Thus, it would be worthy further pursuing the differences of CA916798 function and regulation in LUAD cells with wild-type EGFR versus mutant EGFR.

Together, our work herein demonstrated that CA916798 promoted LUAD cell proliferation and was related with poor prognosis of LUAD patients probably through inhibiting WEE1 expression and subsequent activation of CDK1. Thus, CA916798 could be considered as a promising prognostic marker and a therapeutic target for LUAD.

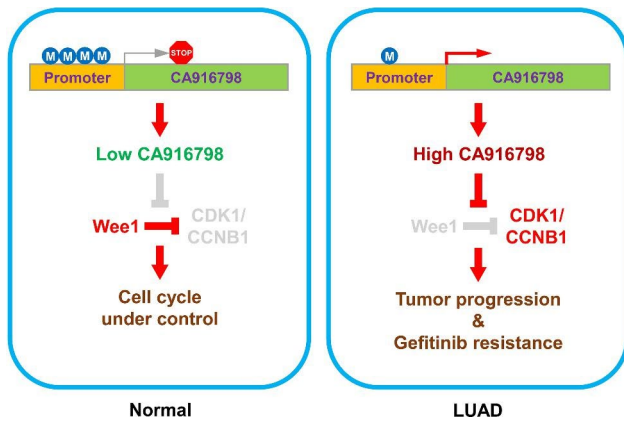


Fig. 7 Targeting CA916798 enhances Gefitinib inhibitory effects on LUAD cells

Schematic diagram of CA916798-mediated progression and Gefitinib resistance of LUAD. In normal lung epithelial cells, promoter of CA916798 gene is hypermethylated and the transcription level of CA916798 is low, which leads to suppression of CDK1 by WEE1 and cell cycle arrest (left panel). In LUAD cells, promoter of CA916798 gene is hypomethylated and the transcription level of CA916798 is dramatically elevated. In this context, CA916798 blocks the inhibition of CDK1 by WEE1 and facilitates cell cycle progression, resulting in LUAD progression and Gefitinib resistance (right panel)

List of abbreviations

LUAD	lung adenocarcinoma
NSCLC	non-small cell lung cancer
TKIs	tyrosine kinase inhibitors
shRNAs	short hairpin RNAs
IHC	immunohistochemistry
IOD	integrated optical density
PBS	phosphate buffer saline
GSEA	Gene Set Enrichment Assay
HE	Hematoxylin-eosin.

Supplementary Information

The online version contains supplementary material available at <https://doi.org/10.1186/s12885-023-10735-3>.

Supplementary Material 1

Acknowledgements

Not applicable.

Authors' contributions

JH and XZ contributed to conception and design of the study. XZ and LZ supervised the project. JH, XLa, and CD provided study materials. JH, XLa, XLi, and HL performed experiments and collected data. JH, PK, ZS, and LZ analyzed data. JH and XZ wrote the manuscript. All authors contributed to manuscript revision, read, and approved the submitted version.

Funding

This work was supported by Project plan for popularization of health appropriate technology of chongqing (2020)stg016 for Xiangdong Zhou.

Data Availability

All data and materials are available in the manuscript. TCGA_LUAD dataset and TCGA_LUAD methylation 450 K datasets are downloaded from <https://xenabrowser.net/>. Kaplan-Meier plotter of Lung Cancer are available at <https://kmplot.com/analysis/>.

Declarations**Competing interests**

The authors have no relevant financial or non-financial interests to disclose.

Ethics approval and consent to participate

The study is reported in accordance with ARRIVE guidelines. The animal experiments were approved by the Laboratory Animal Welfare and Ethics Committee of Army Medical University (AMUWEC20182181). All methods were performed in accordance with the relevant guidelines and regulations.

Consent for publication

Not applicable.

Author details

¹Department of Respiratory medicine, The First Hospital Affiliated to Army Medical University, 29 Gaotanyan Main Street, Chongqing 400038, China

²Institute of Pathology and Southwest Cancer Center, Southwest Hospital, Third Military Medical University (Army Medical University), Chongqing 400038, China

³K2 Oncology Co., Ltd, Beijing 100176, China

Received: 4 November 2022 / Accepted: 13 March 2023

Published online: 23 March 2023

References

1. Barta JA, Powell CA, Wisnivesky JP. Global Epidemiology of Lung Cancer. *Ann Glob Health* 2019, 85(1).

- Siegel RL, Miller KD, Jemal A. Cancer statistics, 2018. *Cancer J Clin.* 2018;68(1):7–30.
- Torre LA, Bray F, Siegel RL, Ferlay J, Lortet-Tieulent J, Jemal A. Global cancer statistics, 2012. *CA Cancer J Clin.* 2015;65(2):87–108.
- Mengoli MC, Longo FR, Frassetto F, Cavazza A, Dubini A, Ali G, Guddo F, Gilioli E, Bogina G, Nannini N, et al. The 2015 World Health Organization classification of lung tumors: new entities since the 2004 classification. *Pathologica.* 2018;110(1):39–67.
- Majem B, Nadal E, Munoz-Pinedo C. Exploiting metabolic vulnerabilities of non small cell lung carcinoma. *Semin Cell Dev Biol.* 2020;98:54–62.
- Blandin Knight S, Crosbie PA, Balata H, Chudzniak J, Hussell T, Dive C. Progress and prospects of early detection in lung cancer. *Open Biol* 2017, 7(9).
- Myers DJ, Wallen JM. Lung Adenocarcinoma. *StatPearls*.edn. Treasure Island (FL); 2022.
- Denisenko TV, Budkevich IN, Zhivotovsky B. Cell death-based treatment of lung adenocarcinoma. *Cell Death Dis.* 2018;9(2):117.
- Sosa Iglesias V, Giuranno L, Dubois LJ, Theys J, Vooijs M. Drug Resistance in Non-Small Cell Lung Cancer: a potential for NOTCH Targeting? *Front Oncol.* 2018;8:267.
- Jao K, Tomasini P, Kamel-Reid S, Korpanty GJ, Mascaux C, Sakashita S, Labbe C, Leighl NB, Liu G, Feld R, et al. The prognostic effect of single and multiple cancer-related somatic mutations in resected non-small-cell lung cancer. *Lung Cancer.* 2018;123:22–9.
- Hsia TC, Liang JA, Li CC, Chien CR. Comparative effectiveness of concurrent chemoradiotherapy versus EGFR-tyrosine kinase inhibitors for the treatment of clinical stage IIIb lung adenocarcinoma patients with mutant EGFR. *Thorac Cancer.* 2018;9(11):1398–405.
- Norouzi S, Gorgi Valokala M, Mosaffa F, Zirak MR, Zamani P, Behravan J. Crosstalk in cancer resistance and metastasis. *Crit Rev Oncol Hematol.* 2018;132:145–53.
- MacDonagh L, Gray SG, Breen E, Cuffe S, Finn SP, O'Byrne KJ, Barr MP. Lung cancer stem cells: the root of resistance. *Cancer Lett.* 2016;372(2):147–56.
- Zhou XD, Liu LZ, Qian GS, Huang GJ, Chen J. [Cloning and sequence analysis of a new, full-length cDNA fragment of drug resistance-related gene in human lung adenocarcinoma]. *Ai zheng = Aizheng = Chinese journal of cancer.* 2002;21(4):341–5.
- Wang HJ, Yang HP, Zhou XD, Dai XT, Chen YF, Xiong W. CA916798 regulates multidrug resistance of lung cancer cells. *Asian Pac J Cancer Prev.* 2011;12(12):3403–8.
- Wang YL, Zhu BJ, Qi ZZ, Wang HJ, Zhou XD. Akt1 enhances CA916798 expression through mTOR pathway. *PLoS ONE.* 2013;8(5):e62327.
- Yang X, Tang C, Luo H, Wang H, Zhou X. Shp2 confers cisplatin resistance in small cell lung cancer via an AKT-mediated increase in CA916798. *Oncotarget.* 2017;8(14):23664–74.
- Duan H, Yang Z, Liang L, Zhou X. CA916798 gene expression is associated with multidrug resistance and predicts progression-free survival in patients with lung cancer. *Oncol Lett.* 2019;18(2):1171–8.
- He J, Lan X, Duan HL, Luo H, Zhou XD. CA916798 affects growth and metastasis of androgen-dependent prostate cancer cells. *Eur Rev Med Pharmacol Sci.* 2018;22(14):4477–87.
- Raspin K, O'Malley DE, Marthick JR, Donovan S, Malley RC, Banks A, Redwig F, Skala M, Dickinson JL, FitzGerald LM. Analysis of a large prostate cancer family identifies novel and recurrent gene fusion events providing evidence for inherited predisposition. *Prostate.* 2022;82(5):540–50.
- Tykodi SS, Fujii N, Vigneron N, Lu SM, Mito JK, Miranda MX, Chou J, Voong LN, Thompson JA, Sandmaier BM, et al. C19orf48 encodes a minor histocompatibility antigen recognized by CD8 + cytotoxic T cells from renal cell carcinoma patients. *Clin Cancer Res.* 2008;14(16):5260–9.
- Song MA, Brasky TM, Weng DY, McElroy JP, Marian C, Higgins MJ, Ambrosone C, Spear SL, Llanos AA, Kallakury BVS, et al. Landscape of genome-wide age-related DNA methylation in breast tissue. *Oncotarget.* 2017;8(70):114648–62.
- Li S, Shi H, Ji F, Wang B, Feng Q, Feng X, Jia Z, Zhao Q, Qian G. The human lung cancer drug resistance-related gene BC006151 regulates chemosensitivity in H446/CDDP cells. *Biol Pharm Bull.* 2010;33(8):1285–90.
- Wang H-J, Yang Z-X, Dai X-T, Chen Y-F, Yang H-P, Zhou X-D. Bisdemethoxycurcumin sensitizes cisplatin-resistant lung cancer cells to chemotherapy by inhibition of CA916798 and PI3K/AKT signaling. *Apoptosis.* 2017;22(9):1157–68.
- Cheng JQ, Wang Y-L, Zhu B-J, Qi Z-Z, Wang H-J, Zhou X-D. Akt1 Enhances CA916798 Expression through mTOR Pathway. *PLoS ONE* 2013, 8(5).
- Qi Z, Wang Y, Zhou X. [CA916798 gene participates in cisplatin resistance of human lung adenocarcinoma A549 cells through PI3K/AKT/mTOR pathway].

- Nan fang yi ke da xue xue bao = Journal of Southern Medical University. 2012;32(9):1290–3.
27. Wee P, Wang Z. Epidermal Growth Factor Receptor Cell Proliferation Signaling Pathways. *Cancers (Basel)* 2017, 9(5).
 28. Reck M, Heigener DF, Mok T, Soria JC, Rabe KF. Management of non-small-cell lung cancer: recent developments. *Lancet*. 2013;382(9893):709–19.
 29. Wo H, He J, Zhao Y, Yu H, Chen F, Yi H. The efficacy and toxicity of Gefitinib in treating non-small cell lung Cancer: a Meta-analysis of 19 randomized clinical trials. *J Cancer*. 2018;9(8):1455–65.
 30. Tan CS, Gilligan D, Pacey S. Treatment approaches for EGFR-inhibitor-resistant patients with non-small-cell lung cancer. *Lancet Oncol*. 2015;16(9):e447–59.
 31. Mok TS, Wu YL, Thongprasert S, Yang CH, Chu DT, Saijo N, Sunpaweravong P, Han B, Margono B, Ichinose Y, et al. Gefitinib or carboplatin-paclitaxel in pulmonary adenocarcinoma. *N Engl J Med*. 2009;361(10):947–57.
 32. Wu SG, Shih JY. Management of acquired resistance to EGFR TKI-targeted therapy in advanced non-small cell lung cancer. *Mol Cancer*. 2018;17(1):38.
 33. Camidge DR, Pao W, Sequist LV. Acquired resistance to TKIs in solid tumours: learning from lung cancer. *Nat Rev Clin Oncol*. 2014;11(8):473–81.
 34. Subramanian A, Tamayo P, Mootha VK, Mukherjee S, Ebert BL, Gillette MA, Paulovich A, Pomeroy SL, Golub TR, Lander ES, et al. Gene set enrichment analysis: a knowledge-based approach for interpreting genome-wide expression profiles. *Proc Natl Acad Sci U S A*. 2005;102(43):15545–50.
 35. Mootha VK, Lindgren CM, Eriksson KF, Subramanian A, Sihag S, Lehar J, Puigserver P, Carlsson E, Ridderstrale M, Laurila E, et al. PGC-1alpha-responsive genes involved in oxidative phosphorylation are coordinately downregulated in human diabetes. *Nat Genet*. 2003;34(3):267–73.
 36. Takizawa CG, Morgan DO. Control of mitosis by changes in the sub-cellular location of cyclin-B1-Cdk1 and Cdc25C. *Curr Opin Cell Biol*. 2000;12(6):658–65.
 37. Wood DJ, Endicott JA. Structural insights into the functional diversity of the CDK–cyclin family. *Open Biology* 2018, 8(9).
 38. Vijayaraghavan S, Moulder S, Keyomarsi K, Layman RM. Inhibiting CDK in Cancer Therapy: current evidence and future directions. *Target Oncol*. 2017;13(1):21–38.
 39. Lynch TJ, Bell DW, Sordella R, Gurubhagavatula S, Okimoto RA, Brannigan BW, Harris PL, Haserlat SM, Supko JG, Haluska FG, et al. Activating mutations in the epidermal growth factor receptor underlying responsiveness of non-small-cell lung cancer to gefitinib. *N Engl J Med*. 2004;350(21):2129–39.
 40. Paez JG, Jänne PA, Lee JC, Tracy S, Greulich H, Gabriel S, Herman P, Kaye FJ, Lindeman N, Boggon TJ, et al. EGFR mutations in lung cancer: correlation with clinical response to gefitinib therapy. *Sci (New York NY)*. 2004;304(5676):1497–500.
 41. Rebuzzi SE, Zullo L, Rossi G, Grassi M, Murianni V, Tagliamento M, Prelaj A, Coco S, Longo L, Dal Bello MG et al. Novel Emerging Molecular Targets in Non-Small Cell Lung Cancer. *International Journal of Molecular Sciences* 2021, 22(5).

Publisher's Note

Springer Nature remains neutral with regard to jurisdictional claims in published maps and institutional affiliations.